

Article

L-Glu Hierarchical Structure Crystallization Using Inorganic Ions

Michal Ejgenberg * and Yitzhak Mastai

Department of Chemistry and Bar-Ilan Institute for Nanotechnology and Advanced Materials (BINA),
Bar-Ilan University, Ramat-Gan 5290002, Israel

* Correspondence: michaldomb@gmail.com

Abstract: Hierarchical organic structures have gained vast attention in the past decade owing to their great potential in chemical and medical applications in industries such as the food and pharmaceutical industries. In this paper, the crystallization of L-glu hierarchical spheres using inorganic ions, namely calcium, barium and strontium cations, is described. The anti-solvent precipitation method is used for the spherical crystallization. The L-glu microspheres are characterized using various techniques, including X-ray diffraction (XRD), scanning electron microscopy (SEM), X-ray photoelectron microscopy (XPS) and polarized microscopy (POM). It is shown that without additives, L-glu crystallizes as flower-like structures, very different from the hierarchical spheres crystallized with the charged additives. Based on our results, we suggest a mechanism for the hierarchical sphere formation based on the crystallization and self-assembly of L-glu in emulsion droplets using charged additives.

Keywords: hierarchical; L-glutamic acid; anti-solvent; precipitation; microspheres; additives



Citation: Ejgenberg, M.; Mastai, Y. L-Glu Hierarchical Structure Crystallization Using Inorganic Ions. *Crystals* **2023**, *13*, 121. <https://doi.org/10.3390/cryst13010121>

Academic Editors: Michael Svård, Rajaboopathi Mani and Zhenguo Gao

Received: 13 December 2022

Revised: 1 January 2023

Accepted: 3 January 2023

Published: 10 January 2023



Copyright: © 2023 by the authors. Licensee MDPI, Basel, Switzerland. This article is an open access article distributed under the terms and conditions of the Creative Commons Attribution (CC BY) license (<https://creativecommons.org/licenses/by/4.0/>).

1. Introduction

Mesocrystals are fascinating crystal structures composed of numerous nano- or micro-sized crystals arranged in a periodic manner [1–7]. They are formed by the self-assembly and organization of very small crystals, as opposed to classical crystallization, which proceeds via molecule-by-molecule crystal growth mechanisms. Mesocrystals were first described about two decades ago by Colfen and Antonietti [7]. Since then, many researchers have reported mesocrystal formation from various inorganic systems, including CaCO₃, BaSO₄ and Fe₂O₃ [8–10]. The early research on mesocrystals was focused on inorganic mesocrystals [11–13]. However, the formation of organic mesocrystals has also been reported [14,15]. For example, Li et al. crystallized hierarchically ordered mesocrystals with a peony-like flower morphology from diphenylalanine [16]. These superstructures were used to construct an anti-wetting surface using fluoroalkylsilane. In another paper, Medina and Mastai crystallized DL-alanine mesocrystals from water/alcohol supersaturated solutions [17]. The DL-alanine structures displayed a needle-like hollow morphology, unlike the needle-like morphology of DL-alanine crystallized from pure aqueous solutions.

Hierarchical organic structures, another class of materials formed by nonclassical pathways, have gained vast attention in the past decade. These organic superstructures are composed of nano- or micro-sized crystals self-assembled in a hierarchical manner. The crystallizations of many organic superstructures have been reported [18–21].

One of the main methods used to synthesize hierarchical crystals is the anti-solvent method [22–25]. Anti-solvent precipitation usually results in the crystallization of nano-sized organic particles with controlled size and morphology. In this method, the material to be crystallized is dissolved in a solvent which dissolves the material very well. Next, an anti-solvent which dissolves the material poorly is added to the mixture. The addition of the anti-solvent induces supersaturation, resulting in precipitation of the solute. Commonly used liquids for the solvent and anti-solvent are water and organic solvents, including

ethanol, acetone, and DMSO. The solvents used in the anti-solvent method must be miscible with each other.

In several cases, the addition of the anti-solvent to the target compound solution results in the formation of a quasi-emulsion of droplets of the target compound and solvent surrounded by anti-solvent. Diffusion of the solvents into one another induces supersaturation of the target compound. Crystallization of the target compound in the solvent drops results in organic hierarchical spherical structures. In many cases, additives are added to the target compound solution to stabilize the target compound self-assembly in the quasi-emulsion drops.

Several research groups have used the anti-solvent precipitation method to crystallize hierarchical organic structures. Colfen et al. crystallized hierarchical microspheres of DL-glutamic acid using polyethylene amine (PEI) as an additive, using the polymer-induced liquid precursor (PILP) process [20]. They were the first group to use an additive which was oppositely charged to the crystallizing material in order to crystallize superstructures. In a later article, our research group crystallized hierarchical microspheres of L-glu using the additive L-arg, based on the opposite charge between the molecules of the crystallizing material and additive, shown by Colfen et al. in their paper [21].

In this paper, the L-glu hierarchical superstructure crystallization using positively charged inorganic ions as additives is described. The anti-solvent precipitation method is used for the spherical crystallization. The L-glu superstructures are characterized using several techniques, including X-ray diffraction (XRD), scanning electron microscopy (SEM), X-ray photo-electron microscopy (XPS) and polarized microscopy (POM). In addition, the effect of the additive concentration on the superstructures is studied. It is shown that without additives, L-glu crystallizes as flower-like structures (low density), very different from the hierarchical spheres (high density) crystallized with the charged additives. Based on our results, we suggest a mechanism for the hierarchical sphere formation based on the crystallization and self-assembly of L-glutamic acid in emulsion droplets using charged ions.

2. Materials and Methods

Sigma-Aldrich (St. Louis, MO, USA): L-glu (purity > 99%), sodium chloride (purity > 99.5%), potassium chloride (purity > 99.5%), calcium chloride (purity > 99.5%), barium chloride (purity > 99.5%), strontium chloride (purity > 99.5%), and ethanol (reagent grade).

Aqueous solutions were prepared using double-distilled water (pH = 5.5).

Crystallization of L-glu in water–ethanol mixtures: 54 mM and 43 mM L-glu aqueous solutions were prepared. For this purpose, 100 mg and 79 mg of L-glu were added to 12.5 mL of water. The solutions were heated (70 °C) and stirred until the L-glu was completely dissolved. The solutions were left to cool to room temperature. A total of 4 mL of the solutions were placed in 50 mL tubes and 4 °C ethanol was added up to the 40 mL line. The tubes were capped and the solutions were shaken by hand and placed in the refrigerator (4 °C) to crystallize (1 day). Filtration or decantation were used to separate the crystals from solution and the crystals were measured by various techniques.

L-glu crystallization with various ions in water–ethanol mixtures:

L-glu (54 mM) was also crystallized with various ions (Ca^{2+} —11 mM and 0.72 mM, Ba^{2+} —5.8 mM and 0.38 mM and Sr^{2+} —7.6 mM and 0.5 mM) under similar conditions.

Characterization: Scanning electron microscope (SEM)—FEI instrument—Inspect S model. Acceleration voltages = 15 kV, 30 kV. X-ray diffraction (XRD)—Bruker AXS D8 Advance diffractometer, $\text{Cu K}\alpha$ ($\lambda = 1.5418 \text{ \AA}$), 40 kV/40 mA, $2\theta = 10^\circ$ to 70° , step size = 0.01° , Time/Step = 0.5 s. Polarized optical microscopy (POM)—BX51-P Olympus microscope, U-AN360-3 polarizer. L-glu morphology calculations—Materials Studio program and Mercury 3.9 software, CIF—ref code LGLUAC11, Cambridge crystallographic database.

3. Results and Discussion

L-glu was crystallized with and without ion additives in order to study the effect of ions on the L-glu crystallization. Figure 1A displays L-glu crystallized in a water–ethanol mixture without additives. As is evident, L-glu crystallizes in very thin plates (ca. 20 μm in length, 250 nm thickness) which together form a flower-like structure. Figure 1B,C show images of L-glu crystallized using sodium and potassium cations, respectively. There is no change in the morphology of L-glu crystallized with sodium ions and there is a small morphological change for L-glu crystallized with potassium ions. The structure is still flower-like. However, the plates making up the flowers are elongated compared to L-glu plates crystallized without ions.

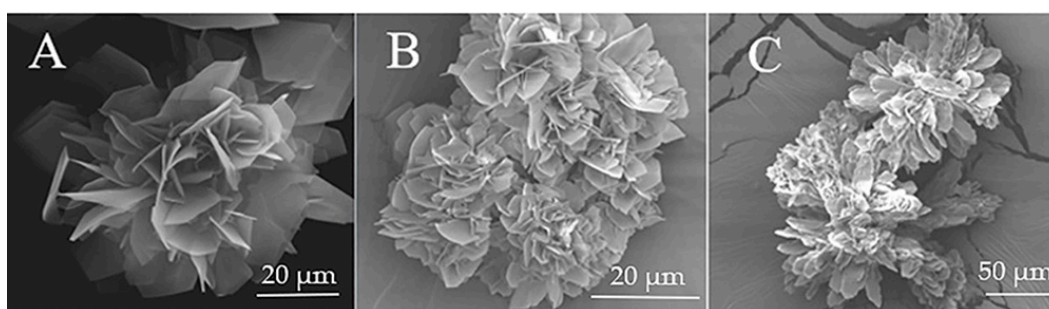


Figure 1. Scanning electron microscopy, pictures of L-glu crystallized without ions (A) and with sodium ions (B) and potassium ions (C) in water–ethanol mixtures.

In addition to SEM measurements, X-ray diffraction measurements were also employed to study the crystal structure of the L-glu flower-like structures and see if there were differences between them. Figure 2 displays X-ray diffraction spectra of L-glu crystallized without ions and with Na^+ and K^+ ions. As can be seen, the same crystal structure is shown in all the spectra. The crystal structure belongs to β -L-glu—a primitive unit cell (space group $\text{P2}_1\text{2}_1\text{2}_1$), $a = 5.159$, $b = 17.30$, $c = 6.948$, and $\alpha = \beta = \gamma = 90^\circ$. Overall, the X-ray diffraction spectra are very similar to one another. There are only very small changes between them.

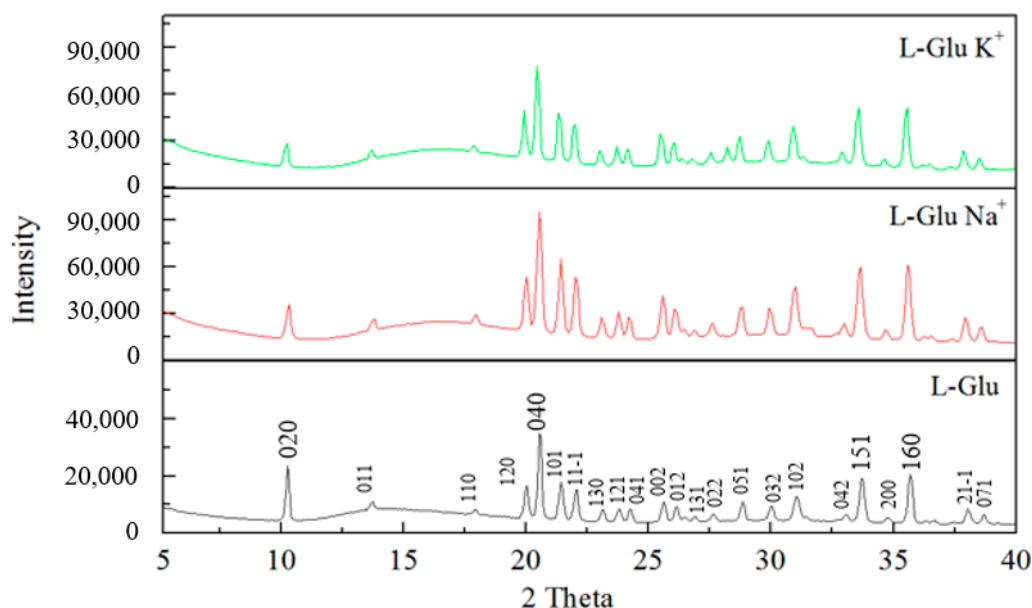


Figure 2. X-ray diffraction spectra of L-glu crystallized without ions, L-glu crystallized with sodium ions and L-glu crystallized with potassium ions.

Figure 3 displays SEM pictures of L-glu crystallized in the presence of barium, calcium, and strontium cations. Figure 3A–D show images of L-glu using high (Figure 3A,B) and low (Figure 3C,D) concentrations of Ba^{2+} . Figure 3E–H show images of L-glu crystallized using high (Figure 3E,F) and low (Figure 3G,H) concentrations of Sr^{2+} . Figure 3I–L show images of L-glu crystallized using high (Figure 3I,J) and low (Figure 3K,L) concentrations of Ca^{2+} . L-glu crystallized using high ion concentrations resulted in dense hierarchical spheres composed of thin plates. L-glu crystallized using low ion concentrations resulted in flower-like structures composed of thin plates. When compared to L-glu crystallized without ions, it is evident that even the low ion concentrations have a strong impact on the morphology of L-glutamic acid. The flowers crystallized in the presence of ions are much more compact and ordered compared to those crystallized without ions. The high ion concentrations have a very strong effect on the morphology and shape of the L-glu crystals.

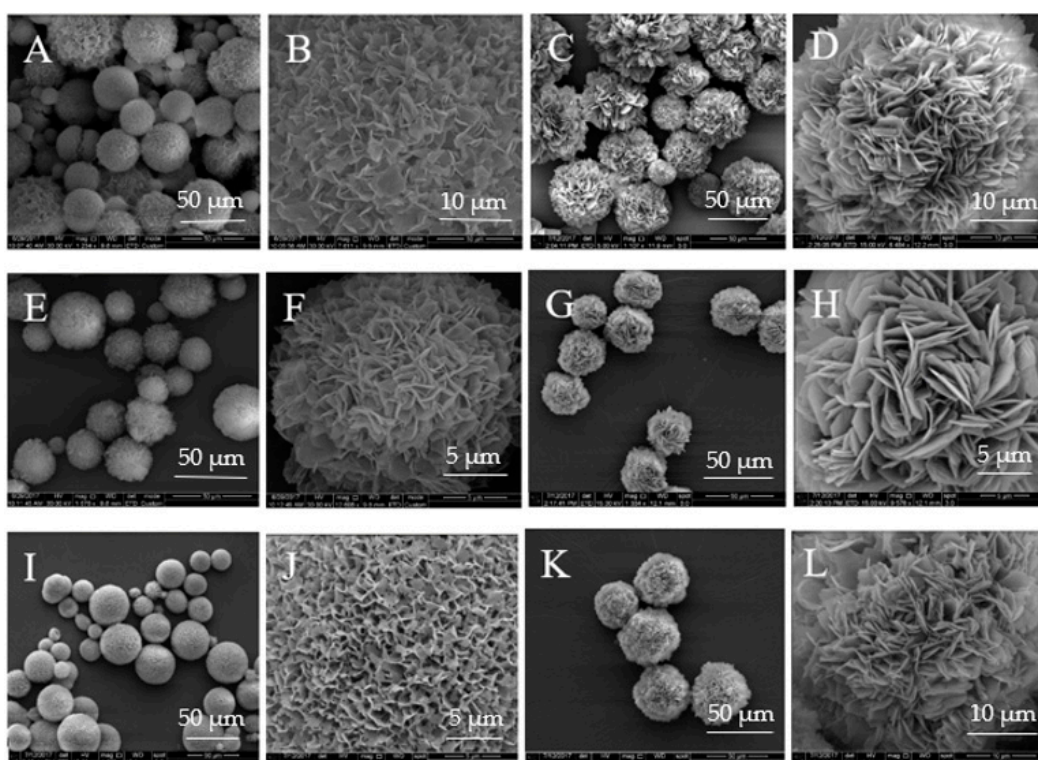


Figure 3. SEM images of L-glu spheres and sphere surfaces crystallized using high (A,B) and low (C,D) concentrations of barium ions, L-glu spheres and sphere surfaces crystallized using high (E,F) and low (G,H) concentrations of strontium ions and L-glu spheres and sphere surfaces crystallized using high (I,J) and low (K,L) concentrations of calcium ions.

XRD spectra of L-glu crystallized without ions and with barium, strontium and calcium ions are shown in Figure 4. It is evident that the same crystal structure is shown in all spectra. The crystal structure belongs to β -L-glu.

Comparing the XRD spectra, it is evident that the addition of ions to the crystallization of L-glu has a major impact on the (020) and (040) peaks. These peaks are markedly reduced in the spectra of L-glu crystallized with ions compared to the L-glu spectrum. The peak intensity reduction is identical for all ions, meaning that the barium, strontium and calcium ions affect the L-glu in the same way. Materials Studio 4.4 software was used in order to model the (020) L-glu plane—Figure 5. It is evident from Figure 5 that carboxylic groups are found protruding from the plane. The carboxylic groups found at the plane add insight to the reason for the reduction of the (020) and (040) peaks. Reduction of the peaks can be caused by electrostatic interactions between the ions and the carboxylic groups. Furthermore, there is also a reduction in the (151) and (160) peaks. In this case, carboxylic

groups are partially exposed at the planes and therefore, the electrostatic interactions are weaker. These findings are in line with previous studies by Colfen et al.

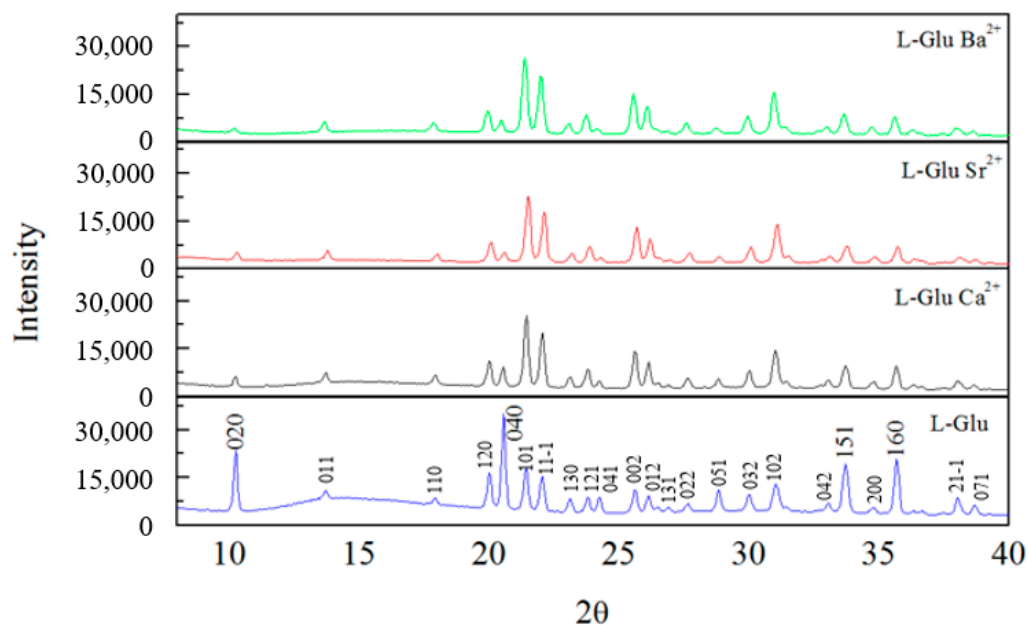


Figure 4. XRD spectra of L-glu and L-glu crystallized with barium, strontium and calcium ions.

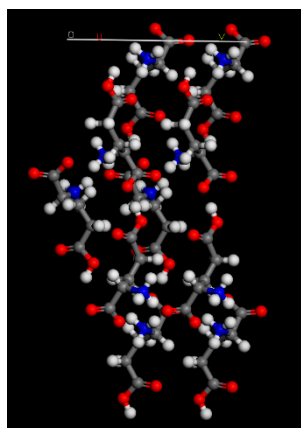


Figure 5. Materials Studio 4.4 (Accelrys)—L-glu (020) crystal plane.

In summary, based on these results, it is shown that bivalent ions have a major effect on the L-glu crystallization in water–ethanol mixtures as opposed to monovalent ions, which do not affect or have a very small effect on the crystallization.

The reason for this may be that during the crystallization and self-assembly of L-glu in the quasi-emulsion droplets, the bivalent ions have a possibility of stabilizing two negatively charged L-glutamic acid molecules, as opposed to the monovalent ions which can stabilize one.

Since the calcium, barium and strontium ions have a very similar effect on the L-glutamic acid spherical crystallization, the next measurements will only be taken in regard to the L-glu spheres crystallized with calcium ions.

It is well known that L-glutamic acid forms complexes with various ions. As a result, the free L-glutamic acid concentration decreases. In order to validate that the hierarchical spherical crystallization is due to electrostatic interactions between the ions and glutamic acid, and not a result of the change in concentration of the free L-glu concentration in the solution, the following experiment was conducted.

As mentioned, 54 mM L-glu crystallized with 11 mM Ca^{2+} ions result in hierarchical spheres. According to Skibsted and Tang, the formation constant of the Ca-L-glu complex equals 5.23 ± 0.17 , 4.54 ± 0.05 or 5.75 ± 0.33 , depending on the pH and ionic strength of the solution [26]. Assuming that all of the calcium ions react with L-glu to form the Ca-L-glu complex, the decrease in L-glu concentration is 11 mM. Therefore, a 43 mM (54 mM—11 mM) L-glu solution of L-glu in H_2O was crystallized without ions. A SEM image of the 43 mM L-glu crystallized without ions appears in Figure 6. As can be seen, the morphology of L-glu crystallized from 43 mM L-glu is very similar to the morphology of L-glu crystallized from 54 mM L-glu and does not result in hierarchical spheres.

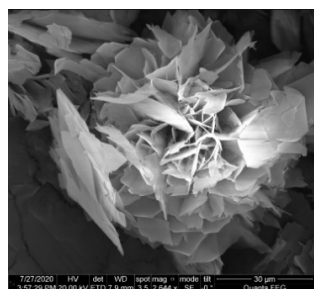


Figure 6. The 43 mM L-glu crystallized in a water–ethanol mixture.

In order to confirm the presence of the Ca^{2+} ion in the spherical L-glu structures, L-glu spheres crystallized from 54 mM L-glutamic acid and 11 mM Ca^{2+} ions were measured by X-ray photoelectron spectroscopy. Figure 7 displays XPS images of the hierarchical spheres. As can be seen, the XPS spectra contain carbon C1s, nitrogen N1s and oxygen O1s peaks, typical of L-glu a. In addition, the spectra also contain a calcium 2p peak, confirming the presence of calcium in the L-glu spheres.

POM (polarized microscope) was used in order to study the internal structure of the L-glu spheres. Figure 8 displays a POM image of L-glu spheres crystallized with Ca^{2+} . As can be seen, the microspheres show clear Maltese crosses when viewed by POM, which suggest radial orientation of the L-glu crystals. L-glu spheres crystallized with barium and strontium ions also show the Maltese crosses when viewed by POM.

As mentioned, the crystallization of L-glu with inorganic ions using the anti-precipitation method (discussed in the introduction) results in hierarchical spheres, very different from the flower-like structures achieved without the inorganic additives. The morphology and shape of the spherical and flower-like structures were studied by SEM. In addition, the XRD spectra of both structures and the Materials studio (020) crystal plane model show us the interactions between the ions and L-glu crystals. The positively charged ions adhere to the crystal planes which expose negatively charged carboxylic acids, causing a decrease in the peaks in the XRD spectrum.

Based on our results, a mechanism for the L-glu hierarchical microsphere formation is suggested and shown in Figure 9. At first, L-glu and the inorganic additive are dissolved in water. Ethanol, the anti-solvent, is added to the aqueous mixture. A quasi-emulsion of water droplets of L-glu and the inorganic additives in ethanol is then formed. The quasi-emulsion forms because the affinity of solute and solvent is greater than the affinity of the solvent and anti-solvent. Here, the solvent forms a bridge between the solute particles and causes them to bind inside the solvent drops. At this point, the solvent and anti-solvent diffuse into one another, and this leads to the supersaturation and rapid crystallization of L-glu into nano- and micro-sized L-glu crystals inside the emulsion drops. L-glu crystallizes inside the emulsion droplets, resulting in the formation of hierarchical spheres. The final step of the mechanism involves the self-assembly, alignment and radial orientation of the nano- and micro-sized L-glutamic acid crystals. The self-assembly of L-glu to hierarchical spheres is aided by the electrostatic interactions between the L-glu and the inorganic ions. When no additives are added, L-glu crystallizes in flower-like structures.

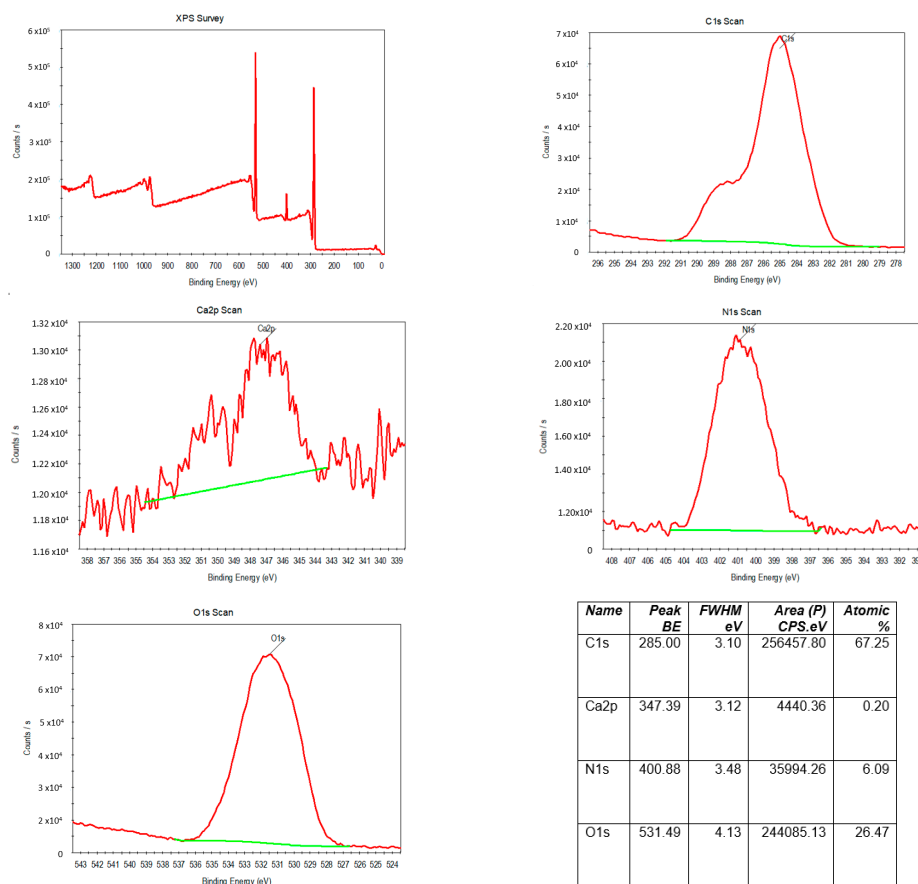


Figure 7. X-ray photoelectron spectroscopy—L-glu spheres crystallized from 54 mM L-glu and 11 mM Ca²⁺ ions.

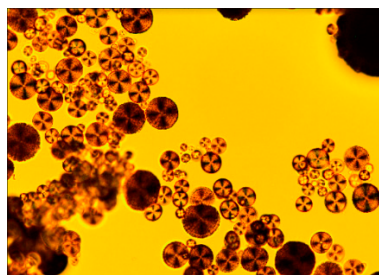


Figure 8. Polarized microscopy image of L-glu spheres crystallized with calcium ions.

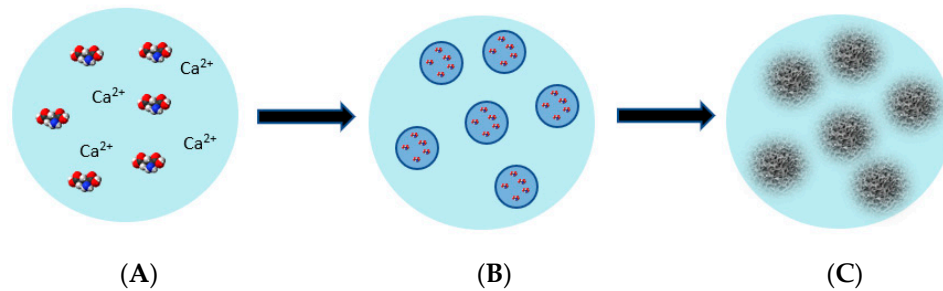


Figure 9. Proposed mechanism: (A) = L-glu and the inorganic additive are dissolved in water, (B) = a quasi-emulsion of drops of water of L-glu and the inorganic additives in ethanol, (C) = crystallization of L-glu inside the emulsion droplets.

4. Conclusions

In conclusion, the formation of L-glu hierarchical spheres using inorganic ion additives, which are oppositely charged to the crystallizing material, is described. The method used is a facile anti-solvent precipitation method. This work demonstrates that charged organic molecules can be crystallized into hierarchical structures by using oppositely charged inorganic additives. We are confident that the synthesis described in this paper can be further extended to achieve hierarchical structures from many other organic materials. A proposed mechanism of the formation of the hierarchical spheres is given. The proposed mechanism is in line with nonclassical models for the nucleation and growth of hierarchical structures. Finally, control over the hierarchical structure formation and crystallization of organic crystals is of great importance for many chemical processes and applications including pharmaceuticals, food additives, fertilizers, and natural materials.

Author Contributions: Conceptualization, M.E. and Y.M.; methodology, M.E. and Y.M.; software, M.E. and Y.M.; writing—original draft, M.E. and Y.M.; data curation, M.E. and Y.M.; writing—review and editing, M.E. and Y.M.; visualization, M.E. and Y.M.; supervision, M.E. and Y.M.; project administration, M.E. and Y.M. All authors have read and agreed to the published version of the manuscript.

Funding: This research received no external funding.

Data Availability Statement: Not applicable.

Conflicts of Interest: The authors declare no conflict of interest.

References

1. Sturm, E.V.; Cölfen, H. Mesocrystals: Past, presence, future. *Crystals* **2017**, *7*, 207.
2. Song, R.Q.; Cölfen, H. Mesocrystals—Ordered nanoparticle superstructures. *Adv. Mater.* **2010**, *22*, 1301–1330. [[CrossRef](#)] [[PubMed](#)]
3. Zhou, L.; O'Brien, P. Mesocrystals Properties and Applications. *J. Phys. Chem. Lett.* **2012**, *3*, 620–628. [[CrossRef](#)] [[PubMed](#)]
4. Ma, M.-G.; Cölfen, H. Mesocrystals—Applications and potential. *Curr. Opin. Colloid Interface Sci.* **2014**, *19*, 56–65. [[CrossRef](#)]
5. Zhou, L.; O'Brien, P. Mesocrystals: A new class of solid materials. *Small* **2008**, *4*, 1566–1574. [[CrossRef](#)]
6. Cölfen, H.; Antonietti, M. *Mesocrystals and Nonclassical Crystallization*; John Wiley & Sons: Hoboken, NJ, USA, 2008.
7. Cölfen, H.; Antonietti, M. Mesocrystals: Inorganic superstructures made by highly parallel crystallization and controlled alignment. *Angew. Chem. Int. Ed.* **2005**, *44*, 5576–5591. [[CrossRef](#)] [[PubMed](#)]
8. Fried, R.; Mastai, Y. The effect of sulfated polysaccharides on the crystallization of calcite superstructures. *J. Cryst. Growth* **2012**, *338*, 147–151. [[CrossRef](#)]
9. Judat, B.; Kind, M. Morphology and internal structure of barium sulfate—Derivation of a new growth mechanism. *J. Colloid Interface Sci.* **2004**, *269*, 341–353. [[CrossRef](#)]
10. Park, G.-S.; Shindo, D.; Waseda, Y.; Sugimoto, T. Internal structure analysis of monodispersed pseudocubic hematite particles by electron microscopy. *J. Colloid Interface Sci.* **1996**, *177*, 198–207. [[CrossRef](#)]
11. Sedlmaier, S.J.; Dennenwaldt, T.; Scheu, C.; Schnick, W. Template-free inorganic synthesis of silica-based nanotubes and their self-assembly to mesocrystals. *J. Mater. Chem.* **2012**, *22*, 15511–15513. [[CrossRef](#)]
12. Tseng, Y.-H.; Lin, H.-Y.; Liu, M.-H.; Chen, Y.-F.; Mou, C.-Y. Biomimetic synthesis of nacrelite faceted mesocrystals of ZnO–gelatin composite. *J. Phys. Chem. C* **2009**, *113*, 18053–18061. [[CrossRef](#)]
13. Duan, X.; Mei, L.; Ma, J.; Li, Q.; Wang, T.; Zheng, W. Facet-induced formation of hematite mesocrystals with improved lithium storage properties. *Chem. Commun.* **2012**, *48*, 12204–12206. [[CrossRef](#)] [[PubMed](#)]
14. Ma, Y.; Cölfen, H.; Antonietti, M. Morphosynthesis of alanine mesocrystals by pH control. *J. Phys. Chem. B* **2006**, *110*, 10822–10828. [[CrossRef](#)] [[PubMed](#)]
15. Su, Y.; He, Q.; Yan, X.; Fei, J.; Cui, Y.; Li, J. Peptide Mesocrystals as Templates to Create an Au Surface with Stronger Surface-Enhanced Raman Spectroscopic Properties. *Chem. A Eur. J.* **2011**, *17*, 3370–3375. [[CrossRef](#)] [[PubMed](#)]
16. Su, Y.; Yan, X.; Wang, A.; Fei, J.; Cui, Y.; He, Q.; Li, J. A peony-flower-like hierarchical mesocrystal formed by diphenylalanine. *J. Mater. Chem.* **2010**, *20*, 6734–6740. [[CrossRef](#)]
17. Medina, D.D.; Mastai, Y. Synthesis of DL-alanine mesocrystals with a hollow morphology. *Cryst. Growth Des.* **2008**, *8*, 3646–3651. [[CrossRef](#)]
18. Ejjenberg, M.; Mastai, Y. Biomimetic crystallization of l-cystine hierarchical structures. *Cryst. Growth Des.* **2012**, *12*, 4995–5001. [[CrossRef](#)]
19. Ejjenberg, M.; Mastai, Y. Hierarchical superstructures of l-glutathione. *Cryst. Growth Des.* **2018**, *18*, 5063–5068. [[CrossRef](#)]
20. Jiang, Y.; Gower, L.; Volkmer, D.; Cölfen, H. Hierarchical DL-glutamic acid microspheres from polymer-induced liquid precursors. *Cryst. Growth Des.* **2011**, *11*, 3243–3249. [[CrossRef](#)]

21. Nemtsov, I.; Mastai, Y.; Ejenberg, M. Formation of hierarchical structures of l-glutamic acid with an l-arginine additive. *Cryst. Growth Des.* **2018**, *18*, 4054–4059. [[CrossRef](#)]
22. Patil, S.; Sahoo, S. Spherical Crystallization: A method to improve tabletability. *Res. J. Pharm. Technol.* **2009**, *2*, 234–237.
23. Kovacic, B.; Vrečer, F.; Planinsek, O. Spherical crystallization of drugs. *Acta Pharm.* **2012**, *62*, 1–14. [[CrossRef](#)]
24. Mahanty, S.; Sruti, J.; Ch, N.P.; ME, B.R. Particle design of drugs by spherical crystallization techniques. *Int. J. Pharm. Sci. Nanotechnol.* **2010**, *3*, 912–918.
25. Teychené, S.; Sicre, N.; Biscans, B. Is spherical crystallization without additives possible? *Chem. Eng. Res. Des.* **2010**, *88*, 1631–1638. [[CrossRef](#)]
26. Tang, N.; Skibsted, L.H. Calcium binding to amino acids and small glycine peptides in aqueous solution: Toward peptide design for better calcium bioavailability. *J. Agric. Food Chem.* **2016**, *64*, 4376–4389. [[CrossRef](#)]

Disclaimer/Publisher's Note: The statements, opinions and data contained in all publications are solely those of the individual author(s) and contributor(s) and not of MDPI and/or the editor(s). MDPI and/or the editor(s) disclaim responsibility for any injury to people or property resulting from any ideas, methods, instructions or products referred to in the content.